08

A 345 GHz waveguide SIS mixer prototype

© *K.I. Rudakov,*[1,2] *A.V. Khudchenko,*[1,2] *V.P. Koshelets*[1,2]

[1] Kotelnikov Institute of Radio Engineering and Electronics, Russian Academy of Sciences,
125009 Moscow, Russia
[2] Astro Space Center of P.N. Lebedev Physical Institute of the Russian Academy of Sciences,
117810 Moscow, Russia
e-mail: rudakov@asc.rssi.ru

Received May 27, 2024
Revised May 27, 2024
Accepted May 27, 2024

Receivers based on the superconductor–insulator–superconductor (SIS) tunnel junction are the most sensitive heterodyne systems for detecting submm and mm-band waves. In this work, we present numerical simulation results and preliminary SIS mixer designs at 345 GHz. The sensitivity of the developed designs to major technological deviations is evaluated. The developed mixer has a high potential to be used on board of the „Millimetron" space observatory as part of an instrument for observations in the Earth-to-space radio-interferometer mode.

Keywords: Superconductor devices, superconductor–insulator–superconductor tunneling transition, sub-THz band receiver systems.

DOI: 10.61011/TP.2024.07.58808.176-24

Introduction

Development of supersensitive sub-mm/mm-band receivers is currently one of the most intensively and successfully developed superconducting electronics areas.

In astronomy, spectral lines of cosmic dust, planet atmospheres, interstellar substance and other extraterrestrial bodies are the main source of data concerning chemical and physical processes of star and planet formation. Mm- and sub-mm wavelength bands are of special interest for astronomic observations, spectral lines of many gases and chemical compounds in „deep space" conditions and radiation peak of interstellar dust and complex organic compounds are concentrated here. This is due to excitation of rotational and vibrational degrees of freedom of complex and simple molecules of stellar and interstellar substances that are in the THz band (for example, H_2O, CH, HCl, NH, OH have absorption lines in sub-THz/THz bands). This band corresponds to the maximum equilibrium radiation for very cold (units of kelvins) objects that are very far from us and their radiation of Earth is weak.

Receiving systems based on the superconductor-insulator-superconductor (SIS) tunnel junction are the most sensitive heterodyne systems for detecting sub-mm/mm band and are used at all modern sub-mm/mm-band astronomic observatories, for example, ALMA (Atacama Large Millimeter Array) located in desert [1], APEX (Atacama Pathfinder Experiment), NOEMA (Northern Extended Millimeter Array) [2–7]. Low operating temperature and high nonlinearity of electric properties of the tunnel junction make it possible to achieve low noise temperatures of receiving elements and, thus, to reduce the time of single observations and increase the observatory performance. Double-sideband (DSB) noise temperature of the mixer is limited by the quantum value $hf/(2k_B)$ [8], where h andk_B are Planck's and Boltzmann's constants, respectively.

In Russian Federation, the „Millimetron" space observatory is developed to be used as an Earth-Space very long baseline interferometer (VLBI) [9,10]. It is designed to study the supermassive black hole metric and environment [11] and to potentially approach the issue of wormhole existence. The „Millimetron" space observatory will be used on halo orbit around Sun-Earth Lagrange point L2. Halo orbit is a quasi-stable orbit in the vicinity of point L2 in a plane perpendicular to the ecliptic . When EHT and Millimetron programs are used together, the expected imaging resolution at 230 GHz may achieve $\Delta\theta \sim 5\,\mu$as [11]. „Millimetron" VLBI receivers will be used for interferometer observations between „Millimetron" and ground stations. to ensure high performance, „Millimetron" VLBI instruments are divided into frequency bands coinciding with ALMA and other ground station frequencies. A site suitable for a submillimeter telescope is now actively sought for in the Russian Federation [12–14].

To create the most high-frequency VLBI channel, 345 GHz SIS receiver is considered as the main candidate. It is planned to use it with 230 GHz [15,16] and 86 GHz channels for black hole shadow observation. Selection of similar frequency bands to develop the Event Horizon Telescope (EHT) project [17] supports research feasibility of creating a high-sensitive receiver for the chosen frequency band in Russian Federation.

Design and engineering of a cryogenic double sideband (DSB) mixer were performed for the 345 GHz SIS tunnel junction receiver. The final objective of the development is to create a fully functional band-splitting receiver that is conceptually similar to ALMA band 9 [18] using the DSB mixer whose design is similar to the 211−275 GHz

solution [19–21]. This will be an assembly based on one-sided (i.e. a waveguide probe and whole integrated circuit are placed only on one side from the waveguide center) or two-sided superconducting mixers in the waveguide unit with high-frequency waveguide hybrid.

1. Design and analysis

To achieve low noise temperature of the tunnel junction receiver element, good agreement shall be provided between the SIS impedance and waveguide at high frequencies and amplifier input impedance at intermediate frequencies (IF), low VHF signal loss level shall be ensured in input waveguide and microstrip paths, and high conversion ratio for the high-frequency (HF) spectrum at IF shall be provided. $Nb-AlO_x-Nb$ tunnel junctions have high nonlinearity of electric parameters and are used to achieve efficient conversion of the high frequency spectrum into the intermediate frequency spectrum.

A $300 \times 600\,\mu$m rectangular waveguide terminated with a waveguide vertical short-circuiting jumper was chosen as an input path. The specimen is placed orthogonally to the wide side of the waveguide as shown in Figure 1, $130\,\mu$m from the waveguide jumper (waveguide end terminated with a solid metal layer). The mixer chip is placed in its own $170 \times 170\,\mu$m waveguide channel and is a planar structure based on the superconducting Nb film in which the SIS junction is included. An aluminum oxide ($Nb-AlO_x-NbN$) SIS tunnel junction with an area of $1\,\mu m^2$, tunnel current density $\sim 9\,kA/cm^2$ and quality parameter defined by $R_j/R_n > 30$, where R_j is the underslot resistance, R_n is the resistance on the normal current-voltage curve (CVC) segment of the SIS tunnel junction, was used as mixer element.

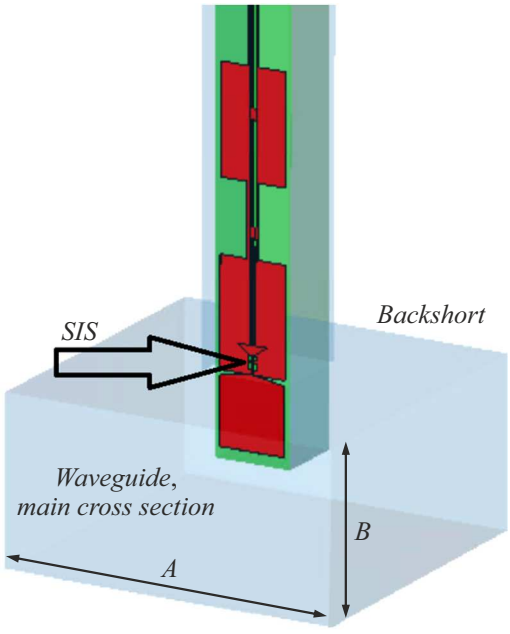

Figure 1. 3D view of a mixer element prototype with one-sided design, i.e. the waveguide probe and the whole integrated circuit are placed only on one side with respect to waveguide center. The arrow shows the tunnel junction location. BxA = $300 \times 600\,\mu$m.

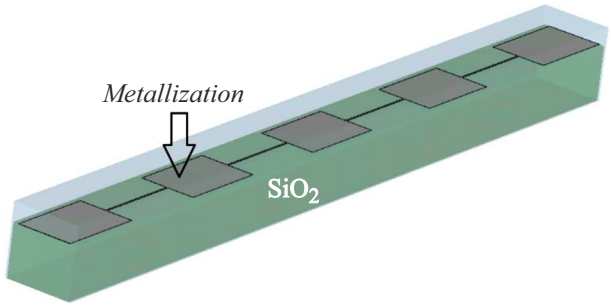

Figure 2. 3D view of the model of reject filter prototype in the Nb layer. The filters are applied to the quartz substrate and are placed in the waveguide channel (Type 1).

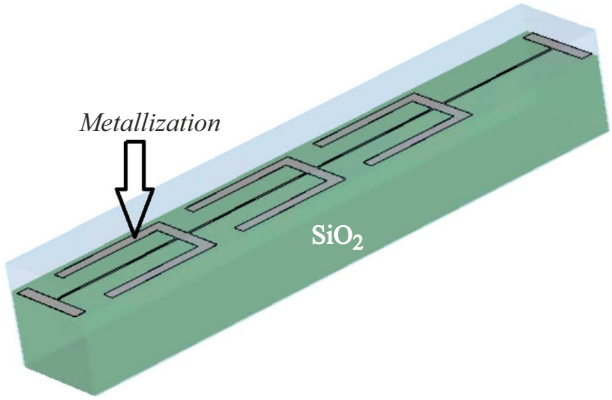

Figure 3. 3D view of the model of reject filter prototype in the Nb layer. The filters are applied to the quartz substrate and are placed in the waveguide channel.

A $125\,\mu$m fused amorphous quartz substrate was used as the chip material to avoid additional polishing. To simplify the calculations, the receiving element had a single-mode design requiring to use the main waveguide dimensions such that the first eigen mode had frequencies about 250 GHz and the second mode had frequencies about 500 GHz. To design the layout shown in Figure 1, it is required not only to match the input radiation in the main waveguide channel, but also to reduce input radiation leakage via the waveguide channel of the prototype, which is a dielectric waveguide. To reduce the leakage, quartz substrates with a permittivity of 3.8, rather than silicon with a permittivity of 12, were used; the waveguide size that ensured the first eigen mode frequency much higher than 350 GHz was also used. To prevent leakage via the metal-plated chip structure, rejection filters are provided. Figures 2 and 3 show various versions of such filters, radiation input-output ports are placed on the waveguide ends.

Type 1 filters (shown in Figure 2) are more convenient for separation of multilayer structure lines, however, they

provide lower, but adequate rejection for mixer operation. Type 2 filters (Figure 3) are more compact, ensure high rejection, but are less convenient in design of multicomponent structures. Therefore, various types of filters were used in [20,21]. Figure 4 shows numerical simulation of filters made in the lower Nb layer metallization.

To input VHF radiation from the waveguide into the planar chip, a quasitriangular waveguide probe is used that is hereinafter referred to as the „probe“. Such type of probe makes it possible to match the high input impedance in the waveguide (hundreds of Ω) with low impedance of microstructures (tens of Ω) on chip. Figure 5 shows the probe impedance distribution on frequency that is equal to approximately 20−i25 Ω.

Figure 1 shows the general layout of the receiving element and its arrangement in the waveguide, and Figure 6 shows a blown-up segment in the vicinity of the tunnel junction. The best match between the tunnel SIS junction impedance and waveguide impedance is ensured by the probe, impedance transformers based on a microstrip lines and asymmetric coplanar transmission line without screen. Transmission lines between the tunnel junctions and waveguide probe are used as transformers. Another asymmetric transmission line

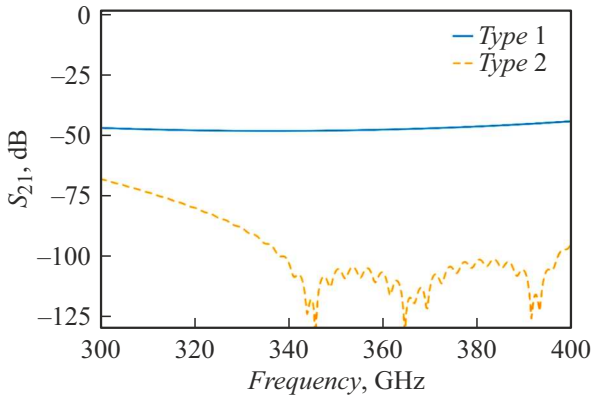

Figure 4. Numerically calculated parameter S21 for Type 1 and Type 2 reject filter prototypes in the lower metallization (Nb) layer. The required transmission level was set to −35 dB.

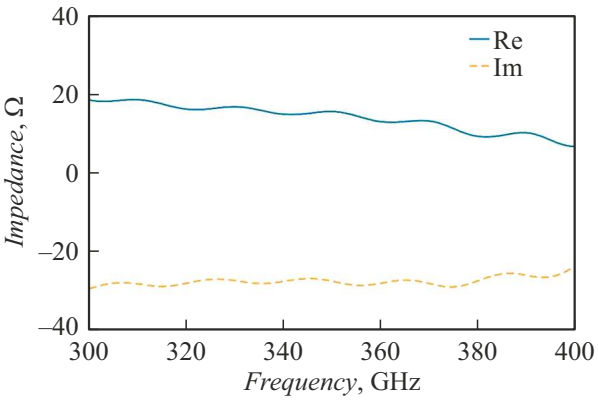

Figure 5. Dependence of the real and imaginary parts of impedance of the quasitriangular waveguide probe on frequency.

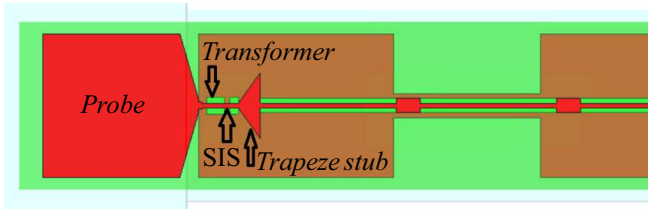

Figure 6. Calculated structure diagram. The arrow shows the SIS junction. The waveguide boundary goes between the probe and reject filter.

Variables of designs $d1$ and $d2$ illustrating Figures 1 and 2

Variables	Design $d1$	Design $d2$
Transformer width, μm	6	5.2
Transformer length, μm	21	19
Trapezoid jumper height, μm	27	24
waveguide probe length, μm	120	102
waveguide probe angle	148°	132°

between the trapezoidal VHF jumper and tunnel junction is addressed as a lumped tuning inductance for capacity offset by the SIS junction at the operating frequency. The SIS junction has a significant capacity (about 80 fF/μm^2) that is able to bridge the input HF signal without additional offset. The trapezoidal jumper is more preferable in the given design that a radial jumper for matching with the low frequency filter (LFF).

The SIS tunnel junction with an area of 1 μm^2 generally makes it possible to match the chip elements using only microstrip lines; however, hybrid structures consisting of microstrip and coplanar lines makes it possible to reduce the spurious capacity and, thus, to expand the IF band. The upper Nb layer also contains reject filters, but due to geometrical limits, they were built in the coplanar asymmetric line (Figure 6), their transmission level is about −30 dB.

The receiving element prototype design required to ensure narrow-band AFR with high match level about 345 GHz. Two designs were made ($d1$ and $d2$) that had different dimensions of transformer elements, tuning elements and probe (see the table), whose theoretical AFR is shown in Figure 7. Design 2 is more narrow-band, but provides better match at the target frequency, only design $d2$ will be addressed hereinafter.

SIS junction is a quantum device electrical specifications of which depend on frequency. Its impedance in the IF band is much higher that in the HF band and may be equal to hundreds of Ω [8]. Together with high capacity of the tunnel junction itself and capacity of tuning structures, this results in considerable reduction of the matching band of the SIS junction and 50 Ohm amplifier input. To expand the IF band, an LC transformer placed on the external PCB in the immediate vicinity of the sample. Figure 8 shows AFR

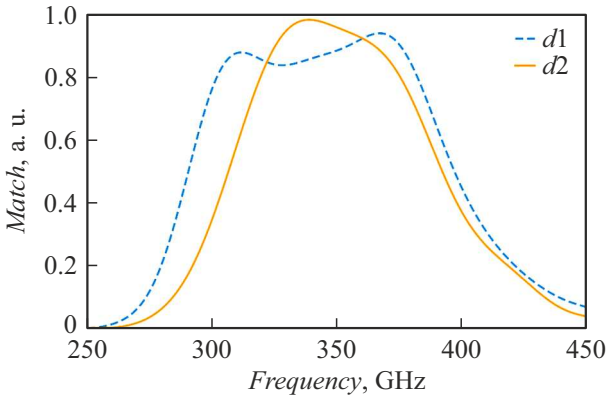

Figure 7. Dependence of power match of SIS junction and waveguide input for two designs ($d1$ and $d2$).

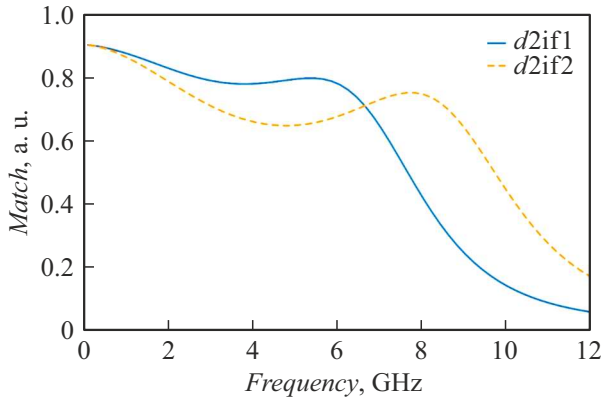

Figure 8. Dependence of power match of the SIS junction and output for amplifier for mixer design $d2$ and two tuning output transformers ($d2$if1 and $d2$if2) in the IF band.

of the receiving element on IF. Another method to expand the IF band is to modify the tunnel junction specifications fundamentally. It is known that the SIS structures based on the Nb–AlN–Nb junctions make it possible to implement high current density and wider IF band, however, the receiving elements on their basis have a lower HF-to-IF conversion ratio [21,22].

2. Analysis of the effect of probable deviations of the main parameters and dimensions

When making the receiving elements and mechanical outfit, minor deviations of the waveguide element dimensions and receiving structure parameters are allowed. When making the planar structure, various process masks of layers shall be aligned, which may result in deviation of the tunnel junction position with respect to the metallization layers. The effect of such deviations on HF AFR is shown in Figure 9.

During SIS formation, minor deviations of the tunnel junction area occur; linear departure of the SIS size by $\sim 0.1\,\mu$m results in SIS junction area change by 20%, the effect of such deviations is shown in Figure 10.

The waveguide unit with the channel for the sample contains deep and thin elements made by milling, estimates of the effect of AFR deviations when making the specified channels are shown in Figure 11, 12.

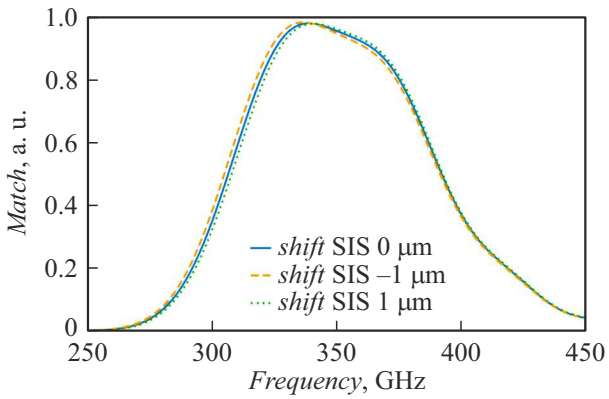

Figure 9. Dependence of power match of SIS junction and waveguide input with SIS junction shift by $1\,\mu$m.

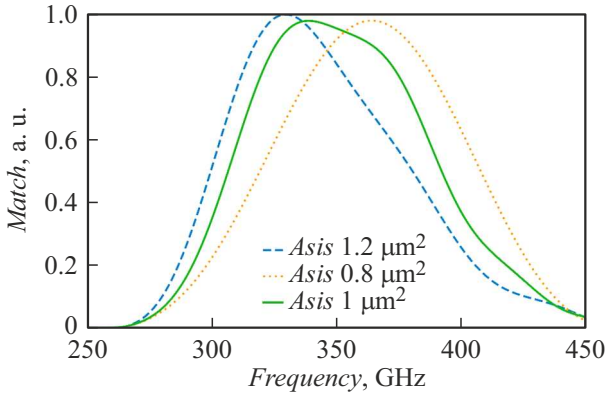

Figure 10. Dependence of power match of SIS junction and waveguide input with deviation from the nominal area by 20%

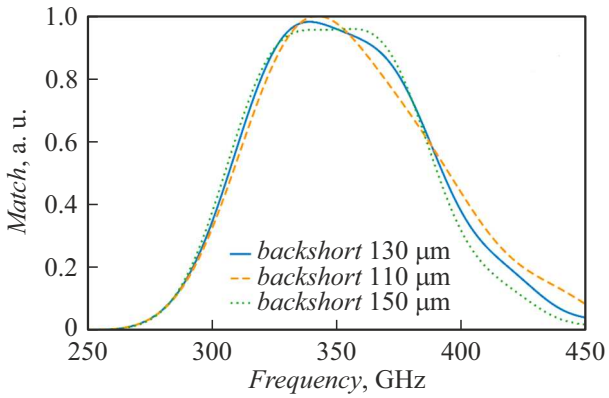

Figure 11. Dependence of power match of SIS junction and waveguide input with waveguide jumper shift by $20\,\mu$m.

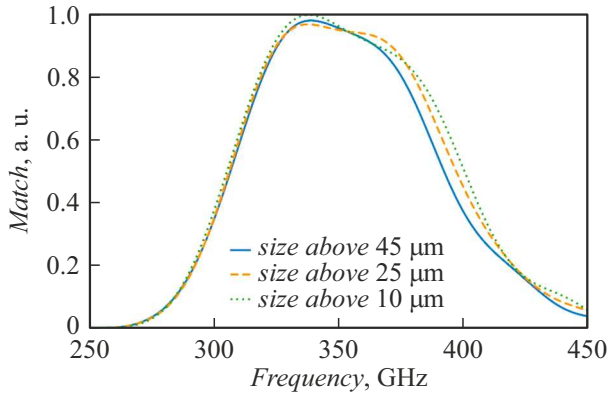

Figure 12. Dependence of power match of SIS junction and waveguide input for design $d2$ when the sample is placed in a more shallow waveguide channel due to milling error. Design clearance between the upper surface of the sample and waveguide unit cover 45 μm.

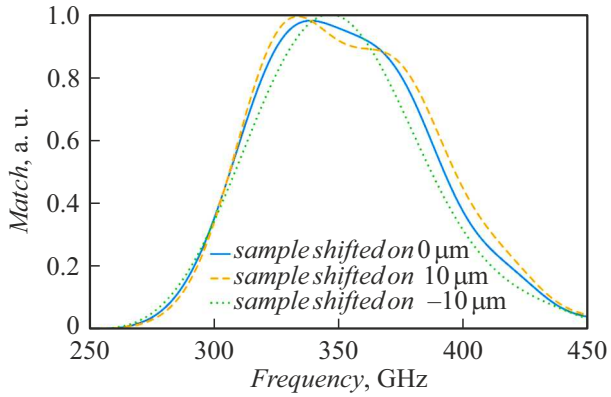

Figure 13. Dependence of power match of SIS junctions and waveguide input for design T2 for sample positioning deviation with respect to the long waveguide wall.

The samples are installed into the waveguide channel using a microscope and a thin needle. During this process, the sample may move inside or outside the main waveguide. Estimate of such deviations is shown in Figure 13.

Thus, minor deviations of the mixing chamber dimensions and sample shifts have no major influence on the mixer performance; SIS junction area departures have the highest influence. Therefore, when making the structures, we design make several junction designs whose diameters differ by 0.1 μm.

3. Stability of the double-sideband mixer (DSB)

To obtain the stability criterium for the DSB mixer in the operating range of 300−370 GHz, Tucker's mixing theory was used [8,23] within low frequencies f_{IF} ($f_{\text{IF}}/f_{\text{HF}} \to 0$). Mixer properties are calculated in the three-port approximation, i.e. it is assumed that current generated on $f_m = f_{\text{IF}} + m f_{\text{IF}}$, $|m| \geq 2$ are short-circuited by the geometrical capacity of the junction. Output admittance Y_{IF} of the SIS mixer is defined as follows

$$Y_{\text{IF}} = \frac{1}{Z_{00}} - Y_L, \tag{1}$$

where Z is the reciprocal of the supplemented matrix Y (for details, see [8,23]), and Y_L is the IF load circuit admittance. Though, it is not obvious from the equation, but Y_{IF} depends on the USB port (IF upper sideband) and LSB (IF lower sideband) admittances, respectively, Y_{UIF} and Y_{LUF}; its value depends on the operating conditions of the pumped SIS, output impedance for the upper sideband Z_s and lower sideband Z_i. Hereinafter, lower indices S and I are used to denote explicitly that the frequency band may be either USB, or LSB. Within $f_{\text{IF}} \to 0$; it can be shown that in the „ideal“ DSB mixer mode [23,24], where

$$Z_S = Z_I \,\text{Im}[Y_{\text{IF}}] = 0.$$

$\text{Re}[Y_{\text{IF}}]$ may become negative depending on the VHF power of SIS tunnel junction pumping by the heterodyne and on Z_S. In this case Y_{IF} is the CVC slope of the „pumped“ SIS junction at constant power of pumping by the heterodyne in the constant bias voltage setting mode. For the purpose of calculations, mixer operation in the DSB mode with $\text{Im}[Y_{\text{IF}}] = 0$ was assumed.

Regions with negative slope on the SIS CVC induced by the effect of the external heterodyne signal are typical for mixers operating in the quantum mode; in contrast, for resistive, so-called classical mixers, condition $\text{Re}[Y_{\text{IF}}] > 0$ is always satisfied. Any device with negative differential resistance is potentially unstable. In the SIS mixer, such instability may result in oscillation in the IF, HF paths or in the SIS operating point setting circuit. In this case, such mixer still may be used, but IF load resistance shall be selected carefully so that $\text{Re}[Y_{\text{IF}}] + \text{Re}[Y_L] > 0$, which is the prerequisite for operation without oscillations [25]. There is a more stringent alternative requirement: $Z_S = Z_I^*$; $\text{Re}[Y_{\text{IF}}] > 0$ for each optimum operating point on CVC with given optimum Z_S that was used for design of single-band receiving mixer element: to chose the optimum operating conditions, the effect of many parameters shall be analyzed, this was addressed in detail by L. D'Addario [25].

The calculation used an operating point in middle of the photon step and the pumping level $\alpha = 1$, because noise temperatures of SIS mixers on this step are minimum or the experimentally measured CVC of the test SIS junction with low leakage. Satisfying the conditions mentioned above for each impedance of structures into which SIS shall be built in and using the three-port approximation of the quantum mixing theory, we have obtained the design restrictions; impedance of the structure that is „seen“ by SIS shall be a little lower than the SIS resistance on the normal CVC branch and shall be mainly capacitive. According to [25], the obtained restrictions are more stringent for SSB than for DSB, and since the designed mixer shall in future work in

a stable manner also in the SSB mode, we need to consider the SSB application as the design stability criterium.

4. Stability of the single-sideband mixer (SSB)

Using the abovementioned Tackers's and Feldman's findings within low frequency range f_{IF} ($f_{\text{IF}}/f_{\text{HF}} \to 0$) for the mixer used in the frequency range of 300−370 GHz, we have specified the stability criterium. Mixer properties were calculation in a three-port approximation. In the SSB mixer, where Y_S and Y_I are different, the real part of the complex output IF admittance (Y_{IF}) may have negative values. For stable operation in this case, care shall be taken when choosing IF load impedance Y_L such that $\text{Re}[Y_{\text{IF}}] + \text{Re}[Y_L] > 0$, which is a prerequisite for operation without oscillations.

For this rule, there is an alternative with a higher „safety margin“, to ensure stable operation, the SSB mixer may be designed using the SIS tunnel junction by choosing Z_I, bias voltages in the constant voltage and VHF pumping power setting mode such that $\text{Re}[Y_{\text{IF}}] > 0$ for Z_S that provides the optimum receiver specifications [25]. A set of assumptions is required for calculation. we assume that these optimum conditions are achieved for the bias voltage in the middle of the first photon step under the action of the VHF heterodyne signal with power corresponding to the pumping level $\alpha = 1$. Moreover, we have assumed that Z_I is reactive ($Z_I = j \times X$ with arbitrary reactive resistance X), that the lower sideband is fully reflected; Z_S corresponds to the normal junction resistance R_n, $Z_S = R_n$. By applying the three-frequency approximation to the quantum mixing theory, using the same SIS CVC as that used in Section 3, we have obtained the restrictions imposed on Z_I so that $\text{Re}[Y_{\text{IF}}] > 0$ at 345 GHz. The obtained values of Z_I normalized to the resistance on the normal branch of CVC (R_n) fall within

$$-j \cdot 4.86 \leq \frac{Z_i}{R_n} \leq +j \cdot 0.16 \qquad (2)$$

and do not depend on R_n. thus, the condition for impedance in LIF Z_I was obtained. We assume that it shall be satisfied by the SSB mixer to ensure the stable operation at 345 GHz. For design, we have selected a matching element structure such that to satisfy the condition. When the same simulation steps were performed in a wider range of 300−370 GHz, it was found that a lower frequency limits the boundaries of the estimated area where the mixer element will work in a stable manner:

$$-j \cdot 3.64 \leq \frac{Z_i}{R_n} \leq +j \cdot 0.13. \qquad (3)$$

Conclusions

A cryogenic DSB mixer using the SIS tunnel junction for 345 GHz was designed and simulated. Two types of filters were designed to provide the rejection level not worse than −45 dB within 300−400 GHz; impedance of the designed waveguide probe was calculated, AFR were obtained for two mixer element designs.

The effect of possible deviations of waveguide element dimensions and receiving structure parameters from the optimum values was estimated numerically; AFR of the designed prototype were calculated considering possible deviations of dimensions and parameters. It is shown that departure of the SIS junction area is most critical, deviation of diameter from the design diameter by 0.1 μm results in the carrier frequency shift by 15−20 GHz.

Stability criteria for mixer elements were used, values obtained from equations (2) and (3) resulted in considerable design restrictions.

The ultimate objective of this development is to create a band-splitting receiver.

Acknowledgments

The authors are grateful to the laboratory team for support, discussion of approaches to easy fabrication of samples and are also grateful to E Tonga, A. Navarrini, A. Baryshev, D. Garret for the interesting discussion during scientific conferences before COVID-19.

Funding

This study was supported by the Ministry of Science and Higher Education of the Russian Federation (Agreement № 075-15-2024-538). Development of superconducting VHF circuit design methods. The study was supported by grant of the Russian Science Foundation № 23-79-00061 (https://rscf.ru/project/23-79-00061/). Development of designs according to process variables, using computational resources.

Conflict of interest

The authors declare that they have no conflict of interest.

References

[1] A. Otarola, M. Holdaway, L.A. Nyman, S.J.E. Radford, B.J. Butler. *Atmospheric Transparency At Chajnantor: 1973-2003* https://library.nrao.edu/public/memos/alma/main/memo512.pdf

[2] A. Wootten, A.R. Thompson. Proc. IEEE, **97** (8), 1463 (2009). DOI: 10.1109/JPROC.2009.2020572

[3] *ALMA Observatory Website* https://www.almaobservatory.org/en/about-alma/

[4] A.M. Baryshev, R. Hesper, F.P. Mena, T.M. Klapwijk, T.A. van Kempen, M.R. Hogerheijde, B.D. Jackson, J. Adema, G.J. Gerlofsma, M.E. Bekema, J. Barkhof, L.H.R. de Haan-Stijkel, M. van den Bemt, A. Koops, K. Keizer, C. Pieters, J. Koops van het Jagt, H.H.A. Schaeffer, T. Zijlstra, M. Kroug, C.F.J. Lodewijk, K. Wielinga, W. Boland, M.W.M. de Graauw, E.F. van Dishoeck, H. Jager, W. Wild. A&A, **577**, A129 (2015). DOI: 10.1051/0004-6361/201425529

[5] R. Güsten, R.S. Booth, C. Cesarsky, K.M. Menten, C. Agurto, M. Anciaux, F. Azagra, V. Belitsky, A. Belloche, P. Bergman, C. De Breuck, C. Comito, M. Dumke, C. Duran, W. Esch, J. Fluxa, A. Greve, H. Hafok, W. Häupl, L. Helldner, A. Henseler, S. Heyminck, L.E. Johansson, C. Kasemann, B. Klein, A. Korn, E. Kreysa, R. Kurz, I. Lapkin, S. Leurini, D. Lis, A. Lundgren, F. Mac-Auliffe, M. Martinez, J. Melnick, D. Morris, D. Muders, L.A. Nyman, M. Olberg, R. Olivares, M. Pantaleev, N. Patel, K. Pausch, S.D. Philipp, S. Philipps, T.K. Sridharan, E. Polehampton, V. Reveret, C. Risacher, M. Roa, P. Sauer, P. Schilke, J. Santana, G. Schneider, J. Sepulveda, G. Siringo, J. Spyromilio, K. Stenvers, F. van der Tak, D. Torres, L. Vanzi, V. Vassilev, A. Weiss, K. Willmeroth, A. Wunsch, F. Wyrowski. APEX: the Atacama Pathfinder Experiment (Proc. 6267, 2006). DOI: 10.1117/12.670798

[6] D. Maier, J. Reverdy, L. Coutanson, D. Billon-Pierron, C. Boucher, A. Barbier. *Fully Integrated Sideband-Separating Mixers for the NOEMA receivers* https://www.nrao.edu/meetings/isstt/papers/2014/2014080084.pdf

[7] P.T.P. Ho, J.M. Moran, K.Y. Lo. ApJ., **616** (1), L1 (2004). DOI: 10.1086/423245

[8] J.R. Tucker, M.J. Feldman. Rev. Mod. Phys., **57**, 1055 (1985).

[9] I.D. Novikov, S.F. Likhachev, Yu.A. Shchekinov, A.S. Andrianov, A.M. Baryshev, A.I. Vasyunin, D.Z. Wiebe, Th. de Graauw, A.G. Doroshkevich, I.I. Zinchenko, N.S. Kardashev, V.I. Kostenko, T.I. Larchenkova, L.N. Likhacheva, A.O. Lyakhovets, D.I. Novikov, S.V. Pilipenko, A.F. Punanova, A.G. Rudnitsky, A.V. Smirnov, V.I. Shematovich. Phys.-Usp., **64** (4), 386 (2021). DOI: 10.3367/UFNe.2020.12.038898

[10] *Millimetron Space Observatory Website*. http://millimetron.ru/index.php/en/

[11] S.F. Likhachev, A.G. Rudnitskiy, M.A. Shchurov, A.S. Andrianov, A.M. Baryshev, S.V. Chernov, V.I. Kostenko. Monthly Notices of the Royal Astronom. Society, **511** (1), 668 (2022). DOI: 10.1093/mnras/stac079

[12] I.I. Zinchenko, A.V. Lapinov, V.F. Vdovin, P.M. Zemlyanukha, T.A. Khabarova. Appl. Sci., **13** (21), 11706 (2023). DOI: 10.3390/app132111706

[13] V.B. Khaikin, V.B. Khaikin, A.Y. Shikhovtsev, A.P. Mironov, X. Qian. Proceed. Sci., **425**, 1 (2022). DOI: 10.22323/1.425.0072

[14] A.Yu. Shikhovtsev, V.B. Khaikin, A.P. Mironov, P.G. Kovadlo. Atmos. Ocean Opt., **35** (2), 168 (2022). DOI: 10.1134/S1024856022020105

[15] K.I. Rudakov, P.N. Dmitriev, A.M. Baryshev, A.V. Khudchenko, R. Hesper, V.P. Koshelets. Radiophys. Quantum El., **62** (7–8), 547 (2019). DOI: 10.1007/s11141-020-10001-7

[16] *ALMA Front End Development* https://zenodo.org/records/5547331≫

[17] M.D. Johnson, K. Akiyama, L. Blackburn, K.L. Bouman, A.E. Broderick, V. Cardoso, R.P. Fender, Ch.M. Fromm, P. Galison, J.L. Gómez, D. Haggard, M.L. Lister, A.P. Lobanov, S. Markoff, R. Narayan, P. Natarajan, T. Nichols, D.W. Pesce, Z. Younsi, A. Chael, K. Chatterjee, R. Chaves, J. Doboszewski, R. Dodson, Sh.S. Doeleman, J. Elder, G. Fitzpatrick, K. Haworth, J. Houston, S. Issaoun, Yu.Y. Kovalev, A. Levis, R. Lico, A. Marcoci, N.C.M. Martens, N.M. Nagar, A. Oppenheimer, D.C.M. Palumbo, A. Ricarte, M.J. Rioja, F. Roelofs, A.C. Thresher, P. Tiede, J. Weintroub, M. Wielgus. arXiv:2304.11188 [kukastro-ph.HE]. DOI: 10.48550/ARXIV.2304.11188

[18] R. Hesper, G. Gerlofsma, F.P. Mena, M.C. Spaans, A.M. Baryshev. *A Sideband-Separating Mixer Upgrade for Alma Band 9*. 20-th Intern. Symp. on Space Terahertz Technology (Charlottesville, 20–22 April 2009) https://www.nrao.edu/meetings/isstt/papers/2009/2009257260.pdf

[19] K. Rudakov, P. Dmitriev, A. Baryshev, A. Khudchenko, R. Hesper, O. Kiselev, V. Koshelets. *Waveguide Receiver Design Prototypes for the 211–275 GHz and 790–950 GHz Frequency Ranges*. 2017 XXXIInd General Assembly and Scientific Symposium of the International Union of Radio Science (URSI GASS, Montreal, QC: IEEE, 2017), p. 1–4. DOI: 10.23919/URSIGASS.2017.8104996

[20] K.I. Rudakov, A.V. Khudchenko, L.V. Filippenko, M.E. Paramonov, R. Hesper, D. Aragão Ronsó da Costa Lima, A.M. Baryshev, V.P. Koshelets. Appl. Sci., **11** (21), 10087 (2021). DOI: 10.3390/app112110087

[21] K. Rudakov. *Development of Advanced Superconductor-Insulator-Superconductor Mixers for Terahertz Radio Astronomy* (University of Groningen, 2021), DOI: 10.33612/diss.174103493

[22] *Band9 Upgrade Study Memo* https://www.eso.org/sci/facilities/alma/developmentstudies/Band9UpgradeStudyReport.pdf

[23] J.R. Tucker. IEEE J. Quant. Electron., **15**, 1234 (1979).

[24] S.-K. Pan, A.R. Kerr. *SIS Mixer Analysis with Non Zero Intermediate Frequencies, Seventh International Symposium on Space Terahertz Technology* (Charlottesville, March, 1996)

[25] L. D'Addario. IEEE Trans. Microwave Theory Techniques, **36** (7), 1196 (1998).

Translated by E.Ilinskaya